parture from the expected behavior, as suggested by the other curves on the figure.

An interatomic potential for the He-He system is calculated using the data in Table I. It is assumed that the general form of the potential is $V(r) = Kr^{-s}$. For such a potential K and s may be found[10] from

$$\sigma(\theta_0, E) = \pi \left(\frac{c_s K}{E \theta_0}\right)^{2/s} \left(1 - \frac{(m_1 + m_2)\theta_0}{m_2 C_s}\right), \quad (3)$$

where θ_0 is the angular resolution, E is the incident energy, and

$$c_s = \frac{(\pi)^{1/2} \Gamma[\frac{1}{2}(S+1)]}{\Gamma(\frac{1}{2}S)} . \quad (4)$$

With the aid of a computer a least-squares fit of the data is made to the above equation and the results are shown in Fig. 6. Curves B and A are, respectively, the potentials for the 0.056°- and 0.260°-resolution data. Curves C and D are the result of calculations done by Phillipson[11] and Abrahamson.[12] Both (E) and (G) are experimental results; E is that reported by Belyaev and Leonas[3] and G is a result from a review article written by Amdur.[13] The present experiment yields potentials whose values are generally higher than those obtained in the earlier experimental studies. At small internuclear separation there is a reasonably good agreement between our results and the theory, while at the larger internuclear separations our potentials lie above those predicted by theory.

[1]I. Amdur, J. E. Jordan, and S. O. Colgate, J. Chem. Phys. **34**, 1525 (1961).

[2]J. E. Jordan and I. Amdur, J. Chem. Phys. **46**, 165 (1967).

[3]Y. N. Belyaev and V. B. Leonas, Dokl. Akad. Nauk SSSR **173**, 306 (1967) [Sov. Phys. Dokl. **12**, 233 (1967)].

[4]A. B. Kannev and V. B. Leonas, Dokl. Akad. Nauk SSSR **162**, 798 (1965) [Sov. Phys. Dokl. **10**, 529 (1965)].

[5]Y. N. Belyaev and V. B. Leonas, Dokl. Akad. Nauk. SSSR **170**, 1039 (1966) [Sov. Phys. Dokl. **11**, 866 (1967)].

[6]E. A. Mason and J. T. Vanderslice, in *Atomic and Molecular Processes*, edited by D. R. Bates (Academic, New York, 1962), Chap. 17.

[7]S. W. Nagy, W. J. Savola, Jr., and E. Pollack, Phys. Rev. **177**, 71 (1969).

[8]S. W. Nagy, S. M. Fernandez, and E. Pollack, Phys. Rev. A **3**, 280 (1971).

[9]D. C. Lorents, W. Aberth, and V. W. Hesterman, Phys. Rev. Lett. **17**, 849 (1966).

[10]E. H. Kennard, *Kinetic Theory of Gases* (McGraw-Hill, New York, 1938), Chap. 3.

[11]P. E. Phillipson, Phys. Rev. **125**, 1981 (1962).

[12]A. A. Abrahamson, Phys. Rev. **130**, 693 (1963).

[13]I. Amdur, in *Atomic Interactions* [A], edited by B. Bederson and W. L. Fite (Academic, New York, 1962), Chap. 3.2.

Scattering between Hg Atoms and Light Atomic Projectiles of keV Energies*

A. van Wijngaarden and W. E. Baylis

Department of Physics, University of Windsor, Windsor, Ontario, Canada

(Received 28 September 1972)

Previously described measurements for the scattering of $^1H^+$, $^4He^+$, $^{11}B^+$, and $^{14}N^+$ ions of energies $9 < E < 75$ keV by a thermal beam of Hg atoms have been extended to smaller angles. Angular distributions for $2.8 < \theta_L < 40$ deg have been measured for the scattering of all projectiles independent of final charge state. Differential scattering cross sections are in approximate agreement with the theory for scattering in a Thomas–Fermi potential over a range of five orders of magnitude. When the cross sections are reduced by the Lindhard procedure, we find that the Thomas–Fermi interaction is a better approximation to the actual potential than the Lenz–Jensen interaction.

I. INTRODUCTION

In a recent publication[1] we presented data for elastic scattering of keV projectiles from Hg atoms. Measured differential-scattering cross sections

for large deflection angles ($\theta_L > 15°$) were found to be in fairly good agreement with theory for the Thomas–Fermi (TF) model of the atom. The present work describes the extension of these experiments to smaller scattering angles ($\theta_L \geq 2.8°$) with
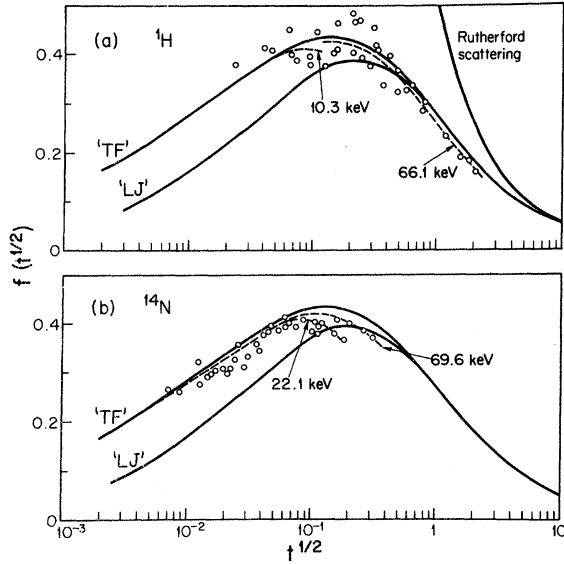
FIG. 1. Scattering functions f vs $t^{1/2}$ (see text) for the TF, LJ, and Coulomb potentials (Rutherford scattering) are from the work of Lindhard et al. (Ref. 5). (a) Reduced-scattering cross sections for $^1H^+$ (circles). Dashed curves represent the actual TF cross sections for $^1H^+$ energies of 10.3 and 66.1 keV. (b) Reduced-scattering cross sections for $^{14}N^+$ (circles). Dashed curves represent the actual TF cross sections for $^{14}N^+$ energies of 22.1 and 69.6 keV.

improved apparatus. The new data cover a sufficiently wide range of angles and energies that it is possible to distinguish between the TF potential and the Lenz–Jensen (LJ) potential. The TF and LJ interactions have recently been discussed in a series of lectures by Sigmund.[2] Both are based on a statistical model of the atom in which electronic charge densities do not exhibit shell structure but decrease monotonically with increasing distance from the nucleus.

First we consider some important aspects of interatomic potentials. In Sec. II apparatus and experimental methods are described. A discussion of the results follows in Sec. III.

A. Thomas-Fermi Potential

In TF theory for an isolated atom the potential is written

$$\frac{1}{e} \, V(R) = \frac{Ze/r_0}{R/r_0} \, \varphi\left(\frac{R}{r_0}\right) \tag{1}$$

with screening radius $r_0 = 0.8853 a_0 Z^{-1/3}$, where $a_0 = 0.529$ Å is the Bohr radius. The screening function $\varphi(x)$ is the solution of the TF equation[3]

$$\varphi'' \equiv \frac{d^2\varphi}{dx^2} = \frac{\varphi^{3/2}}{x^{1/2}}, \tag{2}$$

with boundary conditions $\varphi(0) = 1$ and $\varphi(\infty) = \varphi'(\infty)$

$= 0$. The TF theory has been scaled for a two-atom system[4,5] yielding for the potential energy

$$V(R) = \frac{Z_1 Z_2 e^2/a}{R/a} \, \varphi\left(\frac{R}{a}\right). \tag{3}$$

In this equation R is the internuclear distance and the screening function $\varphi(x)$ is identical to that [Eq. (2)] for a single atom. The screening radius used by Lindhard et al.[5] is

$$a_L = 0.8853 a_0 (Z_1^{2/3} + Z_2^{2/3})^{-1/2}, \tag{4a}$$

and that used by Firsov[4] is

$$a_F = 0.8853 a_0 (Z_2^{1/2} + Z_2^{1/2})^{-2/3}. \tag{4b}$$

These a values are nearly the same when the atomic number Z_1 of the projectile is much less than that (Z_2) of the target atom, and in this work $a = a_L \simeq a_F$.

For a potential of the form above [Eq. (3)] the differential-scattering cross section $d\sigma/d\Omega$ is a function both of the reduced energy $\epsilon = E/(Z_1 Z_2 e^2/a)$, where E is the center-of-mass energy, and of the center-of-mass scattering angle θ. Accurate $d\sigma/d\Omega$ values have recently[1,6] been tabulated for various values of θ and ϵ.

Lindhard et al.[5] have derived an approximation in which the energy and angular dependence is expressed in terms of a single variable $t \equiv \epsilon^2 \sin^2\frac{1}{2}\theta$:

$$\frac{d\sigma}{d\Omega} = \frac{a^2}{8} \, \epsilon^2 \, \frac{f(t^{1/2})}{t^{3/2}}, \tag{5}$$

and they have tabulated $f(t^{1/2})$, the reduced differential-scattering cross section, for the TF potential. When Eq. (5) is inverted and $f(t^{1/2})$ curves are calculated from accurate $d\sigma/d\Omega$ values, it is well known[5,7] that different curves are found at different scattering energies. The discrepancy is apparent in Figs. 1(a) and 1(b), where dashed lines show the small-angle $(\theta \leq 47°)$ Thomas–Fermi $f(t^{1/2})$ curves for ^1H-Hg scattering at center-of-mass energies of 10.3 and 66.1 keV and for ^{14}N-Hg scattering at 22.1 and 69.6 keV. Experimental values (circles) are discussed in Sec. III D.

B. Lenz-Jensen Potential

One of the defects of the TF atom is that it gives a charge density $\rho(R)$ which decreases too slowly (namely, as R^{-6}) at large distances[8] R. The resultant potential falls off as R^{-4} instead of exponentially. A similar objection has been voiced[9] against the TF interaction for a diatomic system.

A variational approach to the statistical theory of the atom has been used by Lenz[10] and Jensen.[11] The electrostatic potential they find can be written in terms of a screening function $\varphi_{LJ}(R/\lambda)$:

$$(1/e) \, V(R) = (Ze/R) \, \varphi_{LJ}(R/\lambda), \tag{6}$$
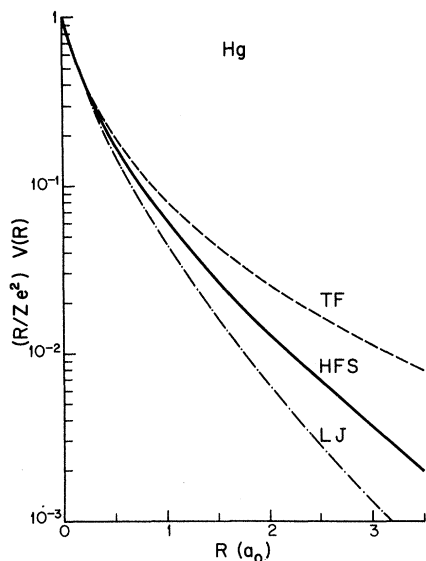
with $R = \lambda s^2$ and

FIG. 2. Screening function $RV(R)/(Ze^2)$ for the electrostatic interaction in Hg $(Z=80)$ in the TF, HFS, and LJ approximations.

$$\varphi_{LJ}(s^2) = e^{-s}(1 + s + 0.3344s^2 + 0.0485s^3 + 0.00265s^4).$$
$$(7)$$

In Fig. 2, the TF and LJ screening functions $\varphi(R)$ [see Eq. (1)] are compared with that from a Hartree–Fock–Slater (HFS) calculation[12] for atomic mercury. The LJ curve is seen to underestimate the HFS $\varphi(R)$ by about the same amount that the TF curve overestimates it. Because of the extended Hg 6s shell, the LJ model potential may be worse for Hg than for many other atoms, yet even Jensen himself[13] has warned against taking the LJ potential seriously at large R. Nevertheless, the LJ potential has been recently advocated[5] as an improvement over the TF potential, and Lindhard[5] has calculated his universal $f(t^{1/2})$ function for the LJ potential (see Fig. 1).

C. Experimental Cross Section

Much of the early work on scattering of keV projectiles has been summarized by Lane and Everhart.[14] Their paper gave justification to the Bohr potential

$$V(R) = (Z_1 Z_2 e^2/R) e^{-R/a} \qquad (8)$$

and to the TF interaction [Eq. (3)]. The experimental data were not sufficiently accurate to make a clear distinction between the two, even though they differ appreciably. In Ref. 1 we demonstrated the superiority of the TF potential to that of Bohr [Eq. (8)].

Similar measurements by Loftager and Claussen[15] for collisions between heavy atoms, in which $Z_1 \sim Z_2$, are in better agreement with the LJ potential.

More recent measurements,[16] however, support the TF interaction rather than the LJ interaction for collisions between Pb and Ar.

In view of the apparent experimental disagreement as well as of the theoretical difficulties[2] involved in computing accurate ion-atom potentials, it seems desirable to extend experimental data so that interaction potentials may be known with greater accuracy.

II. EXPERIMENTAL

The apparatus is an improved version of the one previously described.[1] Inside a target chamber, evacuated to 5×10^{-8} Torr, a beam of singly charged monoenergetic ions is made to interact with a thermal Hg beam at right angles to it. The detection system consists of a channeltron detector (Bendix model No. 4028) that can be rotated about the interaction region. Angular distributions of scattered projectiles are measured with a resolution in the range $\Delta\theta_L \simeq 1.3°$, for the larger scattering angles, to $\Delta\theta_L \simeq 0.7°$, for the smallest deflections. Angular positions θ_L are determined to within an accuracy of $\pm 0.1°$. (The subscript L refers to the laboratory frame of reference.)

A. Thin Film as Energy Filter

Passage of the ion beam through the target chamber produces a variety of energetic projectiles to which the channeltron detector is sensitive. The spectrum of particles contains both high- and low-energy components. We wish to detect only projectiles which have been scattered from the mercury beam. These possess energies comparable to the primary-beam energy. The low-energy component consists of secondary electrons, recoiling target atoms of Hg and of residual gas, and low-energy projectiles that originate in slit scattering events and enter the detector via multiple scattering with the walls of the target chamber. Improved collimation of the incident ion beam has resulted in a reduction by about a factor of 5 in the intensity of the low-energy component. The magnitude of the latter is now comparable to that of the Hg-scattered projectiles.

To prevent detection of the low-energy particles a thin film was placed just in front of the channeltron detector. The film consists of a thin (150-Å) Formvar substrate with a 10-Å Al layer. It was found to be of sufficient thickness to stop the vast majority of the low-energy particles but thin enough so as not to impede the transmission of the high-energy ones.

Projectiles traversing the film undergo many charge-exchange events. Because of this, the charge distribution entering the channeltron does not depend on initial charge. The detection system is therefore equally sensitive to all projectiles,
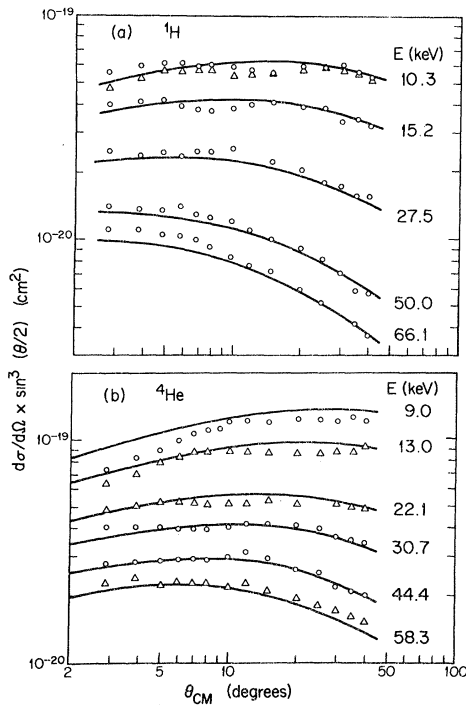
FIG. 3. Angular dependence of the observed scattering cross sections (circles) for (a) protons and (b) He$^+$ projectiles on Hg for several projectile energies. The triangles in (a) are the cross sections for the scattering of H$_2^+$ ions at 20.6 keV. The solid curves are the TF cross sections. Center-of-mass coordinates have been used throughout.

irrespective of their charge after scattering with Hg target atoms.

B. Counting Efficiency

To test the counting efficiency of the detection system several other films with Al layers in the range 50–3000-Å thickness were successively positioned in front of the channeltron detector. One finds that for light atomic projectiles at sufficiently high primary-beam energies the counting rate is independent of film thickness over a relatively large range. This implies that the detection efficiency is independent of energy which is evidence[1] for a high[17] nearly mass-independent[18] efficiency. For the data presented in this work we have assumed the same detection efficiency for all projectiles studied.

C. Scattering Yield and Differential-Scattering Cross Sections

We define the observed scattering yield y as the observed counting rate per unit particle current in the primary ion beam. This yield is related to the cross section $(d\sigma/d\Omega)_L$ as

$$\left(\frac{d\sigma}{d\Omega}\right)_L = \frac{y}{\Delta\Omega(Nt\eta)} \, . \tag{9}$$

Here $\Delta\Omega$ $(4.0\times10^{-4}$ sr) is the solid angle subtended by the detector to the interaction region where the ion beam traverses a thickness t of Hg vapor of density N and η is the counting, i.e., the detection, efficiency. In this work the value of $(Nt\eta)$ is not known but is kept constant so that the previous equation may be written as $(d\sigma/d\Omega)_L = cy$.

D. Calibration with Protons

The proportionality constant c can be found by measuring scattering yields for processes in which $(d\sigma/d\Omega)_L$ is known. For our larger angular deflections of protons (Sec. III A) at higher energies, $t^{1/2}$ is quite large $(t^{1/2}\lesssim 2)$ so that the scattering approaches [Fig. 1(a)] Rutherford scattering. Thus at large $t^{1/2}$, TF theory is quite accurate and the corresponding TF cross sections may be used for calibration. This procedure leads to

$$\left(\frac{d\sigma}{d\Omega}\right)_L = 2.25\times10^{-8}y \ \ (\text{cm}^2) \tag{10}$$

and normalizes our higher-energy proton data to TF theory at large $t^{1/2}$. To compare our results with theory, all cross sections, angles, and energies have been transformed to the center-of-mass system.

III. RESULTS AND DISCUSSION

A. Proton Scattering

The angular dependence of center-of-mass cross sections $d\sigma/d\Omega$ for protons, measured at five primary energies, are shown in Fig. 3, where $\sin^3\frac{1}{2}\theta \times (d\sigma/d\Omega)$ is plotted against θ (center-of-mass values). The θ value assigned to the experimental points corresponds to the actual position of the detector, i.e., the position of the midpoint of the acceptance angle. For a detector with a finite resolution, however, the position that should be assigned is that of the center of gravity of the angular spectrum scattered into it. This position differs from the actual one. It can be shown that the discrepancy is small, smaller than the experimental error $(\pm 0.1°)$ in θ_L. Consequently, no corrections have been applied.

The over-all agreement between experiment and theory (solid curves) for the TF-scattering cross sections[1] is fairly good. Systematic deviations only occur at lower angles where the points lie as much as 15% above the curves. Because of rather large experimental errors [$\pm 5\%$ in $(d\sigma/d\Omega)_L$ and $\pm 0.1°$ in θ_L], the magnitude of the discrepancy cannot be ascertained with confidence.

B. Scattering of H$_2^+$

In TF theory the details of outer-shell effects are not taken into account. These, however, can dominate[2] the interaction, in particular at large
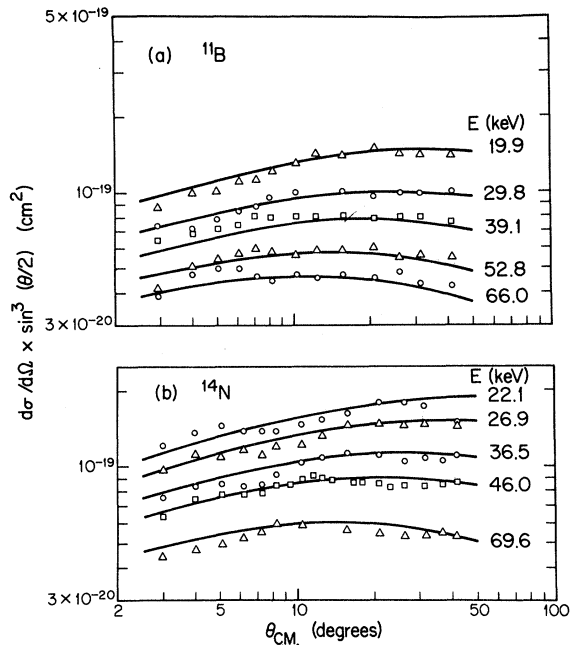
FIG. 4. Angular dependence of the observed scattering cross sections (circles) for $^{11}B^+$ and $^{14}N^+$ projectiles by Hg at five energies. The solid curves are the TF scattering cross sections. Center-of-mass coordinates have been used throughout.

internuclear distances. To investigate whether our scattering cross sections are sensitive to the electronic state of the incident projectile, a beam of H_2^+ ions at an energy of 20.6 keV was used. We find (Fig. 3) that within the limits of experimental error the cross sections (triangles) behave practically as if they arose from the scattering of two protons at half the H_2^+ energy. It thus appears that in the angular range studied the elastic part of the scattering process does not strongly depend on the configuration of outer electrons.

C. Scattering of $^4He^+$, $^{11}B^+$, and $^{14}N^+$

Differential-scattering cross sections for $^4He^+$ are shown in Fig. 3, and those for $^{11}B^+$ and $^{14}N^+$ in Fig. 4. It can be seen that deviations from theory (solid curves) generally do not exceed 15%. There appears to be some structure in the cross sections, but since the resolution $(\Delta\theta_L \sim 1°)$ is not high enough to detect structure over very small angular intervals, only the general features of angular distributions are established here.

It may be noted that the angular distributions for

^{11}B and ^{14}N do not deviate much from horizontal lines, i.e., the observed cross sections vary approximately as $(d\sigma/d\Omega) \propto E^{-1}(\sin\frac{1}{2}\theta)^{-3}$ for small angles. This particular dependence arises from scattering in a $1/R^2$ potential,[5] which approximates the TF potential [Eq. (3)] near $R \sim 2a$. That the approximation holds for such a large range of $d\sigma/d\Omega$ (over four orders of magnitude) may be of interest.

D. Reduced-Scattering Cross Sections

The results for ^1H and ^{14}N discussed in Secs. III A and III C are also presented in Figs. 1(a) and 1(b) in the form of reduced-scattering cross sections. The $f(t^{1/2})$ values have been plotted without specifying the energy at which the actual cross section was measured. To ensure, however, that the various energies are presented with equal weight, about the same number of data points are shown for each of the angular distributions in Figs. 3(a) and 4(b). Similar reduced cross sections are obtained for ^4He and ^{11}B.

The scatter in the points is due to experimental error, to deviations from TF theory including inelastic effects[15] and quantum corrections, and to the fact that the "TF" $f(t^{1/2})$ curve is not unique. The error in $d\sigma/d\Omega$ is $\pm 5\%$ and in θ is $\pm 0.1°$, giving a combined error in $f(t^{1/2})$ of up to ± 15 at the smallest angles. A consequence of the nonuniqueness is that actual TF cross sections fall inside a band (Sec. IA) for which the Lindhard "TF" curve forms an upper bound. A comparison between it and the results is not very meaningful when the band is wide, as is the case near $t^{1/2} \sim 0.2$. At small $t^{1/2}$, on the other hand, the "TF" function is quite accurate and it is in this region that TF theory provides a better over-all approximation to the cross sections than LJ theory.

E. Conclusion

Differential-scattering cross sections for the scattering of $^1H^+$, $^4He^+$, $^{11}B^+$, and $^{14}N^+$ from Hg atoms have been measured for the angular range $2.8° - 38.8°$ at energies below 75 keV. The TF theory provides a good approximation to all measurements over a range of five orders of magnitude. The TF interaction is a better approximation to the actual potential between light atomic projectiles and Hg atoms than the LJ potential.

ACKNOWLEDGMENT

[1]A. van Wijngaarden, B. Miremadi, and W. E. Baylis, Can. J. Phys. **50**, 1938 (1972).

[2]P. Sigmund, Rev. Roum. Phys. **17**, 283 (1972).

[3]See Ref. 1 for an accurate Padé approximant to φ

and for other references.

[4]O. B. Firsov, Zh. Eksperim. i Teor. Fiz. 33, 696 (1957) [Soviet Phys. JETP, 6, 534 (1958)].

[5]J. Lindhard, V. Nielsen, and M. Scharff, Kgl. Danske Videnskab. Selsk. Mat. Fys. Medd. 36, No. 10 (1968).

[6]M. T. Robinson, Oak Ridge National Laboratory Report No. ORNL-4556 (U.S.), 1970 (unpublished), has used Molière and Sommerfeld approximations to the TF potential.

[7]L. Meyer, Phys. Stat. Sol. 44, 253 (1971).

[8]P. Gombas, *Pseudopotentiale* (Springer-Verlag, Wien, 1967), Chap. I, p. 40. See also *Handbuch der Physik* (Springer-Verlag, Berlin, 1956), Vol. 36, p. 109, and *Die Statische Theorie des Atoms und Ihre Anwendungen* (Springer-Verlag, Wien, 1949).

[9]A. A. Abrahamson, Phys. Rev. 130, 693 (1963).

[10]W. Lenz, Z. Physik, 77, 713 (1932).

[11]H. Jensen, Z. Physik, 77, 722 (1932).

[12]We have used the program of J. P. Desclaux [Comp. Phys. Comm. 1, 216 (1969)].

[13]H. Jensen, Z. Physik 101, 141 (1936).

[14]G. H. Lane and E. Everhart, Phys. Rev. 120, 2064 (1960).

[15]P. Loftager and G. Claussen, in *Abstracts, Sixth International Conference on the Physics of Electronic and Atomic Collisions* (MIT Press, Cambridge, Mass., 1969), p. 518.

[16]P. Hvelplund and G. Sørensen, *Abstracts, Seventh International Conference on the Physics of Electronic and Atomic Collisions* (North-Holland, Amsterdam, 1971), p. 1003.

[17]B. Tatry, J. M. Bosqued, and H. Reme, Nucl. Instr. Meth. 69, 254 (1969).

[18]C. N. Burrous, A. J. Lieber, and V. T. Zaviantseff, Rev. Sci. Instr. 38, 1477 (1967).

Molecular Theory of Atomic Collisions: Fine-Structure Transitions

F. H. Mies

National Bureau of Standards, Washington, D.C. 20234

(Received 11 September 1972)

The theory of fine-structure transitions in atom-atom collisions is formulated in terms of the molecular states of the diatomic collision complex. The Born–Oppenheimer (BO) electronic wave functions are implicit functions of the interatomic coordinate R, and the molecular theory is analogous to the "perturbed-stationary-state" method. Expansion in *molecular* channel states incorporates the effects of polarization, exchange, and valence forces on the electronic portion of the scattering wave function and embodies the "adiabatic" contribution of the entire set of closed-channel excited states that are generated in the more usual asymptotic-atomic-state expansion. The channel states are expressed explicitly in terms of the body-fixed molecular wave functions, and the resultant interaction matrix elements in the close-coupling scattering formalism are related to the molecular potentials. The theory is developed specifically for proton collisions with the fluorine atom in its ground $^2P_{j, m_j}$ state, with explicit account being taken of the spin-orbit splitting between the $j = 3/2$ and $j = 1/2$ multiplet states. Use is made of the accurate $HF^+(^2\Pi)$ and $HF^+(^2\Sigma)$ wave functions calculated by Wahl, Julienne, and Krauss. These molecular states asymptotically approach $H^+ + F(^2P)$, and accurate quadrupole and induced-dipole interaction parameters which describe the asymptotic interaction potentials are obtained from the calculations. Estimates are made of the BO coupling terms and they are found to be negligible compared to the spin-orbit couplings. In the following paper close-coupling calculations are made of the cross sections for the fine-structure transitions $(j, m_j \rightarrow j', m_j)$.

I. INTRODUCTION

The wave functions that describe the scattering between two atoms A and B are equivalent to the continuum wave functions of the diatomic molecule AB, and it is well recognized[1] that the adiabatic electronic states of the molecule form a useful basis with which to formulate the low-energy scattering problem. This is known as the perturbed-stationary-state (pss) method and is expected to be superior (i.e., more rapidly convergent) to the usual expansion in asymptotic atomic states since the molecular Born–Oppenheimer (BO) states are implicit functions of the interatomic distance R

and incorporate the effects of polarization, electron exchange, and valence forces. The theory has been applied extensively[1-3] but has suffered from lack of accurate molecular potentials, and/or use of approximate techniques in treating the coupling between the adiabatic states. It is only recently that some of these limitations have been removed[4-6] and the increasing availability of accurate molecular wave functions suggests the need to approach the molecular theory of atomic collisions with increased rigor. To this end it is advantageous to treat the collisions between a proton H^+ and a ground-state fluorine atom $F(^2P)$. This is one case which goes beyond simple elastic scattering that can be treated